

Acute exposure to copper oxide nanoparticles impairs testicular function and sperm quality in adult male albino rats

Lamiaa Hassan¹, Ibrahem M. A. Hasan², Zeinab Al-Amgad³ and Hassan Ahmed^{1*}

¹Department of Physiology, Faculty of Veterinary Medicine, South Valley University, Qena 83523, Egypt, ²Department of Chemistry, Faculty of Science, South Valley University, Qena 83523, Egypt, ³Veterinary National Services, PhD in Veterinary Pathology and Clinical Pathology, Faculty of Veterinary Medicine, South Valley University, Qena, Egypt.

Abstract

Copper oxide nanoparticles (CuO NPs) are metallic nanoparticles fulfilling several functions such as good conductivity, catalyst, used in sensors and energy storage devices, and antibacterial characteristics. However, the cytotoxicity and particular mechanisms of exposure to CuO NPs on male testicular function are still elusive. In the current study, seventy-five mature male albino rats received single doses of 0, 100, 200, 1000, and 2000 mg/kg CuO NPs by oral gavage. Blood and epididymal semen as well as testicular tissue were collected 2, 8, and 15 days after administration. Serum testosterone level, sperm motility, count, morphology, viability, and gonadosomatic index (GSI) were assessed at the same time; histological structure of the testes was examined. The result revealed that CuO NPs significantly reduced serum testosterone levels, suppressed sperm concentration, and significantly elevated abnormal and dead sperm percent. Furthermore, testicular tissue showed degeneration of germ, Sertoli, Leydig cells, and spermatocytes with the incidence of vacuolation and inflammatory cell infiltration. In conclusion, CuO NPs exert adverse and irreversible effects on testicular function and sperm physiological characteristics; these harmful effects were markedly observed after administration of high doses of CuO NPs.

Keywords: Copper oxide nanoparticles, Testosterone, Gonadosomatic index, Sperm morphology, Sperm viability.

DOI: 10.21608/svu.2023.226884.1288 Received: August 2, 2023 Accepted: January 16, 2024

Published: February 17, 2024

*Corresponding Author: Hassan Ahmed

E-mail: Hassan-younes@vet.svu.edu.eg

Citation: Hassan et al., Acute exposure to copper oxide nanoparticles impairs testicular function and sperm quality in adult male albino rats. SVU-IJVS 2024, 7(1): 1-21.

Copyright: © Hassan et al. This is an open access article distributed under the terms of the creative common attribution license, which permits unrestricted use, distribution and reproduction in any medium provided the original author and source are created.

Competing interest: The authors have declared that no competing interest exists.



Introduction

Nanotechnology is a rapidly advancing science that contributes to numerous industrial, agricultural, and medicinal applications. The small size of nanoparticles (NPs) (1-100 nm) gives them unique properties such as transport and crossing the biological barriers including blood brain and testicular barriers (Laurent *et al.*, 2008). Even so, the impact of nanoparticles on general health conditions and physiological functions is still not completely elucidated. Copper (Cu) is one of the most important micronutrients for cellular function, enzymatic activity, normal physiological processes, carbohydrate metabolism, and antioxidant defense (Chen *et al.*, 2022). There are many routes by which Cu enters the body including inhalation of polluted air, consumption of food and water, and dermal contact. Although, copper is useful for the body. If its intake over the body adaptation limit, it accumulates in the body producing deleterious effects including impairment of the liver, kidney, immune system, and gastrointestinal functions, neurological diseases as well as reproductive dysfunction (Jomova *et al.*, 2022).

Copper oxide nanoparticles (CuO NPs) are widely used in abundant industrial implementations such as lubricants, polymers, plastics, textiles, metallic coating, antimicrobials, and home appliances. However, they have been blamed for their contribution to the toxicity of living bodies (Gallo *et al.*, 2018). Owing to its overuse and small size, CuO NPs easily transported through tissues and cross the brain and testicular barriers accumulating in the target organs such as the brain, liver, and kidney producing dysfunction of these organs manifested by neurotoxicity (Assy *et al.*, 2019). All the

mentioned adverse effects of CuO NPs were mediated by the generation of oxidative stress including lipid peroxidation and DNA damage subsequently cytotoxicity and apoptosis. As previously mentioned, CuO NPs easily cross the blood testicular barrier consequently; the male reproductive system is one of the target organs that can be adversely affected depending on the dose and exposure period. The perturbation of male reproduction results in the production of ROS which is the main contributor to damage of spermatogenesis, steroidogenesis, hypothalamic-pituitary-gonadal axis regulation and sperm maturation and fertility (Samrot and Noel Richard Prakash, 2023).

The current study is an endeavor to clarify the effect of acute exposure to CuO NPs in different single doses (0, 100, 200, 1000, and 2000 mg/kg) on adult male albino rat's reproductive performance by assessment of testicular hormone, estimation of sperm characters by semen analysis, calculation of gonadosomatic index, and histopathological examination of testicular tissue.

Materials and methods

Ethical approval

The experimental protocol was carried out according to the ethical research Committee of the Faculty of Veterinary Medicine, South Valley University who approved the methodology of the current study (Approval number: 26/16/11.2021). The management and care of the experimental animals were carried out following the Egypt National Institutes of Health Guidelines for the Care and Use of Laboratory Animals. The animals were kept for one week as an adaptation period to the

new environment before starting the experiment.

Chemicals and reagents

Both sodium hydroxide (99% purity) and copper (II) acetate monohydrate ($(\text{CH}_3\text{CO}_2)_2 \cdot 2\text{H}_2\text{O}$ (98% purity) are analytical-grade chemicals that were obtained from Merck (Merck KGaA, Darmstadt, Germany) and used exactly as directed. Banana (*Musa acuminata*) was purchased from the local market, Qena governorate, Egypt. In this experiment, all used solutions were prepared using double-distilled (DD) water.

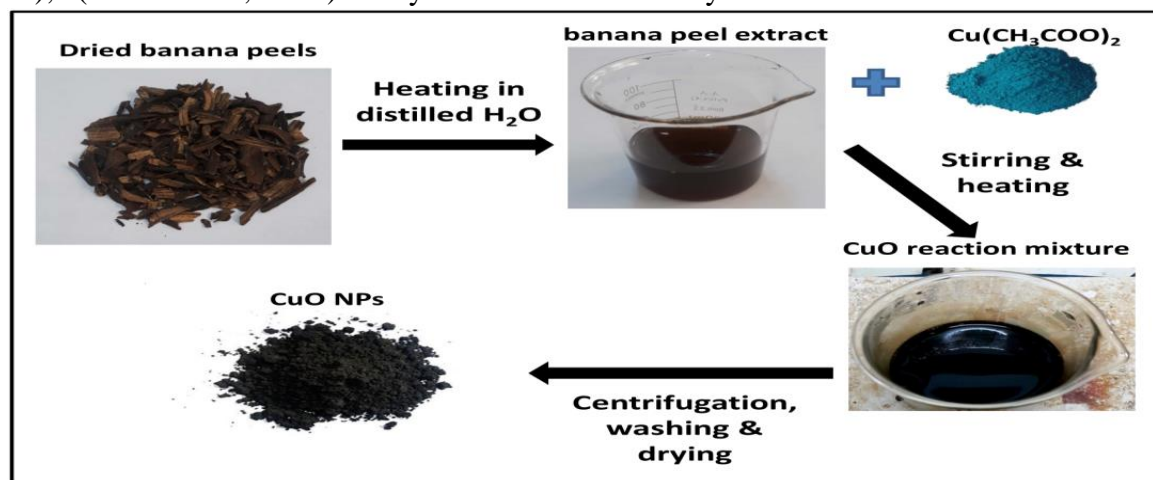
Making extract from banana peels

Banana peels were washed with tap water, rinsed in distilled water, and then let to dry in the sun for 15 days. In a Pyrex glass beaker, 300 mL of distilled water with 20 grams of dried banana peels were boiled for 15 minutes and then kept overnight at room temperature. The boiled mixture was exposed to double filtration by using glass wool and Whatman No. 1 filter then the extract was kept at 4°C until use.

Copper oxide nanoparticles (CuO NPs) green synthesis and characterization

Scheme 1 depicts the schematic representation of the synthesis that was performed using our prior methodology with certain adjustments (Hasan et al. (2021); (Hasan et al., 2022)). Sixty mL of

banana peel extract (BPE) and 5 grams of $\text{Cu}(\text{CH}_3\text{CO}_2)_2 \cdot 2\text{H}_2\text{O}$ (1:12 m/v) were mixed while stirring and heating for 5 minutes. When the black CuO had completely precipitated, 60 mL of 5% NaOH was added to the reaction mixture in parts, and the reaction was then constant for a further 30 minutes. The CuO NPs were separated by centrifugation at 6,000 rpm for 12 minutes, followed by three separate washes in DD H_2O and ethanol, and kept for drying at 80°C for 3 hours. Using a pestle and mortar, the finished mixture was mashed and kept in an airtight container. The obtained CuO NPs were examined by using a powder x-ray diffractometer (X'Pert3 Powder, PANalytical, The Netherlands) to evaluate phase structure and size analysis. The diffractometer was operated at 40 kV voltage and 30 mA current, using monochromatic radiation ($\text{Cu-K}\alpha$, 1.5406 Å) with a diffraction angle in the 20-80° range. Moreover, the Scherrer equation ($D = K/\cos$) was used to calculate the crystallite size. Besides, Fourier-transform infrared spectroscopy (FTIR) spectra (Shimadzu, Kyoto, Japan) were collected to assess the potential function of phytochemicals in the synthesis of CuONPs . Finally, a transmission electron microscope (TEM) examination was used to verify the size and form of the CuO NPs



Scheme 1: Green synthesis of CuO NPs.

Animals

Seventy-five healthy adult male albino rats (Wistar strain) aged 12 to 14 weeks and weighing 150 to 250g were purchased from the Laboratory Animal House, Faculty of Medicine, Sohag University, Sohag, Egypt. Rats were carried to the Physiology Department, Faculty of Veterinary Medicine, South Valley University, Qena, Egypt. They managed in

Experimental procedure

After a week of acclimatization, the rats were distributed into five groups (15 rats for each), each group subdivided into three subgroups (5 rats for each). The experiment lasted 15 days. The following treatments were given to the rats according to OECD (2001):

Group I: served as a control and treated with a single dose of deionized water orally with oral gavage.

Group II: treated with a single dose of 100 mg/kg BW from CuO NPs orally administered with oral gavage.

Group III: treated with a single dose of 200 mg/kg BW from CuO NPs orally administered with oral gavage.

Group IV: treated with a single dose of 1000 mg/kg BW from CuO NPs orally administered with oral gavage.

Group V: treated with a single dose of 2000 mg/kg BW from CuO NPs orally administered with oral gavage.

CuO NPs dry powder was mixed with deionized water to make a homogenous suspension, which was then sonicated for ten minutes at room temperature. To prevent the NPs from aggregating before delivery, the period between preparation and oral administration was kept to a maximum of 20 minutes. Oral gavage was used to provide doses to all rats, with a dosage amount of 10 mL/kg body weight.

Blood collection

sterile plastic cages within the standard healthy environment (23-25°C, 40-70% humidity, and with a 12-h light/12-h dark cycles). The rats were maintained on a regular chow diet and clean tap water *ad libitum*. The cages and glass water bottles were cleaned, and the bedding was changed twice per week. The experimental rats were adapted for one week to the new environment before starting the experiment.

One subgroup (5 rats) from each treatment group was anesthetized with diethyl ether at 2, 8, and 15 days following the oral gavage of deionized water or CuO NPs after the experiment was completed. Blood samples from the retro-orbital venous plexus were taken, centrifuged for 15 minutes at 3000 rpm, and the sera were kept at -80°C until the testosterone hormone assessment.

Testosterone assessment

The frozen serum was defrosted, and serum testosterone levels were evaluated using enzyme-linked immunosorbent assay (ELISA) kits according to the manufacturer's instructions (Monocent, Inc., CA, USA) Catalogue NO. (EL1-1263) by using a microplate reader (Infinite 50, Männedorf, Switzerland) at wavelength 450 nm (Tietz, 1995).

Testes collection

Rats were sedated with an intraperitoneal dose of sodium thiopental (50 mg/kg bw) at the end of the experimental period. One subgroup from each group was slaughtered at 2, 8, and 15 days following the administration of CuO NPs. The testes were excised out quickly for calculation of the gonadosomatic index, epididymal semen analysis, and histological examination.

Calculation of gonadosomatic index

The average weight of the excised testes (g) and final body weight (g) were

obtained then the gonadosomatic index was calculated according to Kumari and Singh (2013) as the following formula:

$$\frac{\text{Testes weight (g)}}{\text{Final body weight (g)}} \times 100$$

Semen analysis

After the slaughtering and testes excision, semen was collected from the epididymis and diluted in warmed physiological saline at 37°C according to D'Souza (2003). According to Seed *et al.* (1996), sperm motility was evaluated by placing a drop of semen on a warmed, dry, and clean slide. To assess the sperm's vitality (dead and live percent), one drop of semen was applied simultaneously on a dry mixed with drop of wormed (37°C) eosin - Nigrosin stain 1:1 freshly prepared and spread slid, the percent of dead and live sperms were calculated (Esteso *et al.*, 2006). According to Wyrobek and Bruce (1975), sperm abnormalities were detected by combining one drop of diluted semen with an Eosin stain the percent of normal and abnormal sperms were calculated. Finally, the epididymal sperm concentration was assessed by dilution with sodium bicarbonate solution and formalin, followed by sperm counting using Neubauer hemocytometer as described by (Srinivasulu and Changamma, 2017).

Histological examination

The testicular tissue samples were quickly removed following the method described by Kittel *et al.* (2004), fixed in (10%) neutral buffered paraformaldehyde, treated using the standard paraffin embedding procedure, and then sectioned at a thickness of around 5 µm. Tissue slices were stained with Hematoxylin and Eosin (H&E) (Gamble, 2008) and then inspected under the light microscope for any changes to the normal histological structure.

Statistical analysis

The obtained data were statistically analyzed using GraphPad Prism 8 (GraphPad Software, San Diego, California, USA). The results were presented as mean ± standard error of the mean (SEM), and Tukey's multiple comparisons test was used to examine differences between groups after a two-way analysis of variance (ANOVA). Values of $P < 0.05$ were deemed significant.

Results

Physical characteristics of CuO NPs

The x-ray diffract-meter (XRD) of the green synthetic CuO NPs is shown in Figure 1A to demonstrate the phase and crystal structure. The crystalline nanoparticles depicted multiple diffraction peaks at 2θ values of 32.48, 35.63, 38.86, 48.84, 53.27, 58.39, 61.55, 66.35, 68.23, 72.63, 74.35, and 82.71 matching the appropriate Miller indices of (110), (11-1), (200), (20-2), (020), (202), (-113), (310), (220), (221), (004) and (222). These results corresponded with COD file no. 9016326 (Asbrink and Waskowska, 1991) (volume-81.5, system-monoclinic, space group- C 1 c 1 (9), cell parameter a = 4.6927, b = 3.4283, c = 5.137, a/b = 1.36881, c/b = 1.49841). Using the Scherrer equation, the CuO NPs had an average crystallite size of 14.50 nm (Table 1).

The role of phytochemicals in the BPE extract in the reduction of copper salt and capping of the resultant nanoparticles was investigated using FTIR spectroscopy. Comparative FTIR spectra show absorption peaks in the 400–4000 cm^{-1} wavenumber range as found in our previous work (Mohamed *et al.*, 2023).

Major peaks in the BPE FTIR spectra were found between 3418 and 1623 cm^{-1} . These peaks are referred to as hydroxyl group in-plane bending vibrations, O-H expansion, and maybe amide N-H group

stretching. The C-N (unsaturated) and C-H bending vibrations are shown by the peaks at 2931 and 1055 cm^{-1} , respectively. CuO NPs' spectra showed peaks at 3426 and 1632 cm^{-1} , which correspond to the OH's stretching and bending, respectively as shown in our previous work (Mohamed *et al.*, 2023). Additionally, 632 and 539 cm^{-1} were found to have distinctive Cu-O peaks (Maulana *et al.*, 2022; (Vinothkanna *et al.*, 2022). The lowering and capping effects of

organic moieties in BLE are confirmed by our data. A transmission electron microscope was used to examine the morphology of the as-produced CuO NPs (Figure 1A). The picture displays clusters of rod-shaped CuO NPs with typical lengths of 18 nm and 5 nm widths (Table 1). The crystalline structure of the CuO NPs is demonstrated by the selected area electron diffraction (SAED) pattern (Figure 1B).

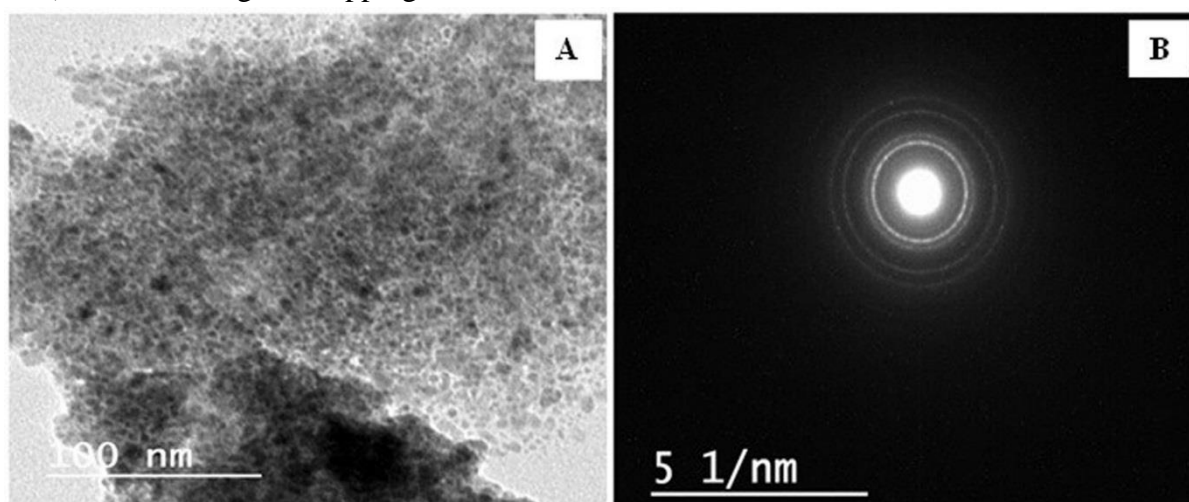


Figure 1: (A) TEM image and (B) SAED pattern of CuO NPs

Sample	Crystallite size (XRD)	Crystallite size (TEM)	Surface area	Mean pore diameter	Pore volume, $\text{cm}^3 \text{g}^{-1}$	
					BET	NLDFT
CuO BPE	14.50 nm	5.21 nm	$8.839 \text{ m}^2 \text{g}^{-1}$	8.9135nm	0.0197	0.0197

Table 1: Physical properties of the manufactured CuO NPs

The material surface area on which the reactions take place has an impact on the physicochemical activity. Higher activity often correlates with greater surface area. N₂ adsorption/desorption analysis at 77 K has been used to examine the CuO NPs' Brunauer-Emmett-Teller (BET) surface area and Non-Local Density Functional Theory/Grand Canonical Monte Carlo (NLDFT/GCMC) pore size. CuO NPs' N₂ sorption isotherm at P/P₀ = 0.982 (Figure 2A) is categorized by the IUPAC as Type IV with a single point final plateau and Type H3 hysteresis loop, which denotes non-rigid

gathers of mesoporous particles leading to slit-shaped pores (Thommes *et al.*, 2015). Additionally, the NLDFT/GCMC pore size distribution curve (Figure 2B) estimate of the mean pore diameter of 8.9135 nm confirms the mesoporous structure of CuO NPs. The N₂ molecule's cross-section area of 16.2 Å was used to determine the BET-specific surface area, which came out at 8.839. Both BET and NLDFT/GCMC also indicate that the total pore volume at saturation pressure is 0.0197 $\text{cm}^3 \text{g}^{-1}$ (Table 1).

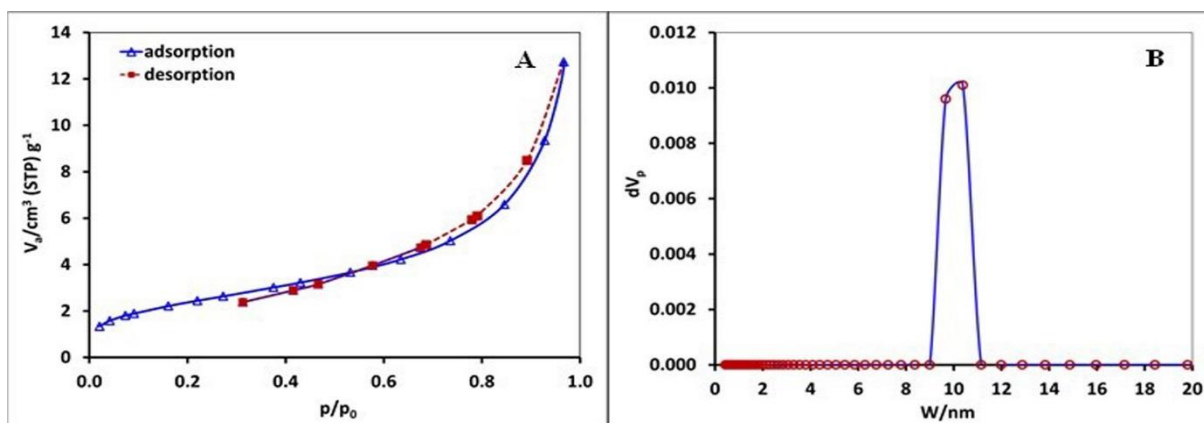


Figure 2:(A) Adsorption/desorption isotherm and (B) NLDFT/GCMC pore size distribution analysis of CuO NPs

Acute exposure to CuO NPs declines serum testosterone level.

Figure (3) depicts serum testosterone (ng/mL) levels in control and treated rats after 2, 8 and 15 days after CuO NPs administration. Two- and eight-day post-CuO NPs administration, 100, 200 and 1000mg-treated groups showed a tenuous decline in serum testosterone levels. The values of serum testosterone for the 100 mg-treated group were (8.49 ± 1.41 and 7.34 ± 0.78 , respectively). The 200 mg-treated group was (7.63 ± 1.23 and 7.25 ± 0.31 , respectively). For the 1000 mg-treated group were (7.65 ± 0.47 and 7.63 ± 0.63 , respectively) compared with the corresponding control (9.02 ± 0.63 and 8.12

± 1.07 , respectively). Fortunately, serum testosterone levels recovered in all three former groups after 15 days from administration (8.94 ± 0.87 , 9.67 ± 1.21 , and 9.72 ± 0.98 , respectively in the 3 groups) to be around the control level (8.88 ± 0.48). On the contrary, after administration of 2000 mg of CuO NPs, treated rats showed a significant decrease in testosterone levels. Two and eight days after administration, the values of treated rats were (3.05 ± 0.55 and 2.91 ± 0.71 , respectively) compared with control and other treated groups. Although the level of testosterone significantly reduced (5.66 ± 0.14) 15 days after CuO NPs administration.

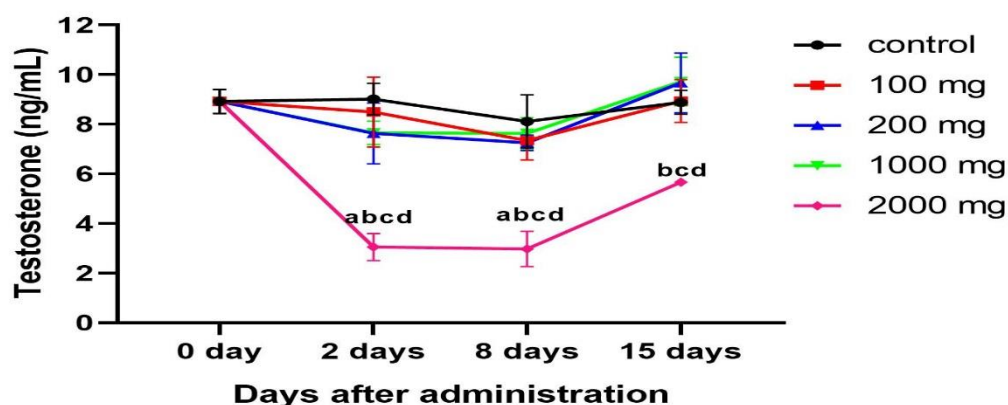


FIGURE 3: THE SERUM TESTOSTERONE LEVEL AT DIFFERENT TIME POINTS (2, 8 AND 15 DAYS) AFTER THE ORAL ADMINISTRATION OF CuO NPs IN CONTROL AND TREATED GROUPS. DATA ARE EXPRESSED AS THE MEAN \pm SEM ($N = 5$, TWO-WAY ANOVA) ^A $P < 0.05$, vs. CONTROL, ^B $P < 0.05$, vs. 100 MG, ^C $P < 0.05$, vs. 200 MG AND ^D $P < 0.05$, vs. 1000 MG.

Copper oxide nanoparticles alter the physiological characteristics of the epididymal sperm

Complete semen analysis that monitors normal properties of the epididymal sperm was described in Figure (4). Although the sperm motility (%) adversely diminished in all treated groups after CuO NPs administration, this decline was non-significant after 2 and 8 days after administration compared with the corresponding control. Furthermore, the sperm motility improved after 15 days and upward direction toward the control level as shown in Figure (4A).

Sperm count ($10^6/\text{ml}$) in all treated groups showed a variable deteriorated degree after CuO NPs administration in a time-dependent manner. Groups that received 100, 200, and 1000 mg CuO NPs disclosed a non-significant decrease in sperm count (152.00 ± 31.53 , 156.00 ± 16.31 , and 108.00 ± 20.35 , respectively after 2 days), (153.60 ± 9.06 , 147.00 ± 7.16 and 96.80 ± 16.65 , respectively after 8 days) and (156.80 ± 12.08 , 141.50 ± 9.43 and 114.80 ± 6.45 , respectively after 15 days) compared with corresponding control (178.00 ± 19.34 , 161.80 ± 10.79 and 167.80 ± 19.05 , respectively after 2, 8 and 15 days). However, an obvious decline in sperm count was observed after administration of the higher dose of CuO NPs (2000 mg). As treated groups showed a significant decrease in sperm count 2 and 8 days after administration (75.83 ± 8.41 and 73.00 ± 5.14 , respectively) and a non-significant decline (92.67 ± 6.26) after 15 days (Figure 4B).

One of the most affected physiological parameters is sperm morphology owing to CuO NP-induced testicular toxicity. Herein, the abnormal sperm percent adversely affected by CuO

NPs depends on the dose and time elapsed after administration as shown in Figure 4C. After 2 days of administration, groups administered 100 mg of CuO NPs showed a non-significant increase of abnormal sperm percent (21.40 ± 3.98) compared with control and other treated groups. However, the 200 mg-treated group disclosed a significant elevation of abnormal sperm percent (27.00 ± 1.92) compared with the control (11.60 ± 2.91). Likewise, the group that received 1000 mg revealed a significant elevation of abnormal sperm percent (31.00 ± 3.45) compared with the control and 200 mg-treated groups. Surprisingly, the abnormal sperm percent significantly increased (41.00 ± 1.87) to 4-fold compared with the control, 2-fold compared with the 100 mg group, and 1.3-fold compared with 200 and 1000 mg-treated groups. Although abnormal sperm percent decreased non-significantly 8 days post administration compared with those after 2 days, two groups exposed a non-significant significant rise of abnormal sperm percent (16.80 ± 2.22 and 20.60 ± 2.29 , respectively) compared with control (11.00 ± 2.39) and other treated groups after 8 days. Additionally, the higher dose of CuO NPs depicted an unfavorable effect on sperm abnormality more than the lower dose. For instance, 8 days after administration of 1000 mg, abnormal sperm percent significantly elevated (33.20 ± 3.54) compared with control and 100 mg groups and non-significantly compared with other groups. Also, a high percent of sperm abnormality was shown after administration of 2000 mg of CuO NPs after the same time point (37.80 ± 3.44) compared with the control and other treated groups. Within the same trend, after 15 days 100 and 200 mg-treated groups showed a non-significant increase of abnormal sperm percent

(20.80 ± 2.22 and 23.00 ± 3.38 , respectively) compared with control (12.00 ± 1.76) and other treated groups. However, abnormal sperm percent elevate significantly (29.60 ± 2.25) after administration of 1000 mg CuO NPs compared with control and after administration of 2000 mg (33.40 ± 4.81) compared with control and 100 mg group and non-significantly compared with other groups.

Similarly, sperm viability was adversely affected by CuO NPs in a dose- and time-elapsed-dependent manner. Dead sperm percent increased proportionally with the dose while, the percentage tended to be improved longer post administration as described by Figure 4D. After 2 and 15 days, all treated groups showed significant elevation in dead sperm percent after 2 days (18.80 ± 3.06 and 19.20 ± 3.81 , respectively in 100 mg group, 20.40 ± 3.59 and 19.60 ± 1.81 , respectively in 200 mg group,

34.60 ± 3.41 and 30.00 ± 1.70 , respectively in 1000 mg group, 40.20 ± 1.28 and 31.40 ± 3.33 , respectively in 2000 mg group) compared with the control (7.20 ± 1.39 and 9.60 ± 1.89 , respectively). In addition, the altered effect of CuO NPs at higher doses (1000 and 2000 mg) in the same time points was markedly observed, and treated rats that showed a significant increase in dead sperm percent compared with 100 and 200 mg. At the same time, after 8 days, 100 and 200 mg-treated rats revealed a significant elevated (22.40 ± 2.06 and 26.60 ± 2.06 , respectively) in dead sperm percent compared with the control (8.40 ± 1.54). Besides, the 1000 mg group depicted a significant increase in dead sperm percent (33.00 ± 1.14) compared with the control and 100 mg-treated group. Also, rats received 2000 mg showed significant elevation in dead sperm percent (39.40 ± 3.50) compared with the control, 100 and 200 mg administered groups.

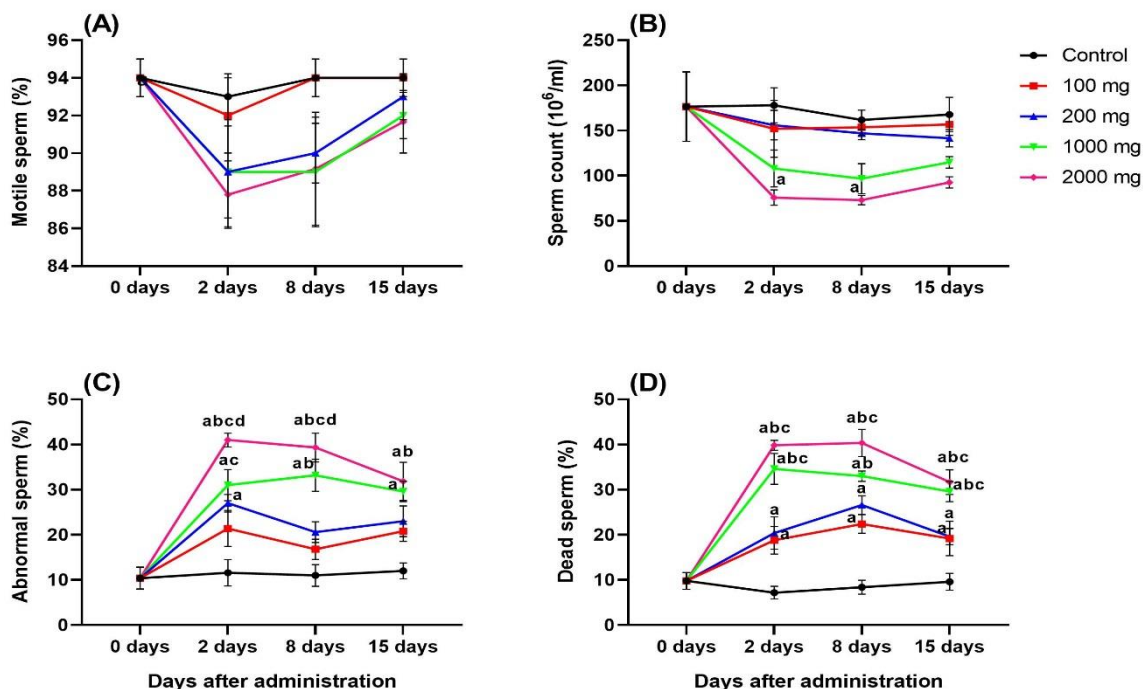


FIGURE 4: SEMEN ANALYSIS AT DIFFERENT TIME POINTS (2, 8 AND 15 DAYS) AFTER THE ORAL ADMINISTRATION OF CuO NPs IN CONTROL AND TREATED GROUPS. (A) SPERM MOTILITY (%). (B) SPERM COUNT. (C) ABNORMAL SPERM (%). (D) DEAD SPERM (%). DATA ARE EXPRESSED AS THE MEAN \pm SEM ($N = 5$, TWO-WAY ANOVA) ^a $P < 0.05$, vs. CONTROL, ^b $P < 0.05$, vs. 100 MG, ^c $P < 0.05$, vs. 200 MG AND ^d $P < 0.05$, vs. 1000 MG.

Figure 5 showed the live and dead sperms under the light microscope after staining with Nigrosin-Eosin stain. The head of the dead sperm appeared stained with Eosin which freely crossed the cell membrane and stained the sperm head.



FIGURE 5: A LIVE AND DEAD SPERM MICROPHOTOGRAPH AFTER THE ORAL ADMINISTRATION OF CuO NPs IN CONTROL AND TREATED GROUPS. DEAD SPERM STAINED BY EOSIN STAIN (ARROW) WHILE; LIVE ONES APPEAR NON-STAINED (ARROWHEAD). EOSIN-NIGROSINE STAIN. (MAGNIFICATION=100X).

Furthermore, Figure 6 exhibited the normal (figure 6A) and abnormal sperms (figure 6B-H) under the light microscope after being stained by eosin stain. Normal sperm is characterized by a hock-shaped

However, the live sperm cell membrane kept the properties of selective permeability and prevented the eosin stain to transport inside the cytoplasm so, the head of a live sperm appeared unstained.

head and tail while the abnormal sperm forms are represented by a coiled tail, detached head, compact or broken head, immature sperm, and sperm tail without head.

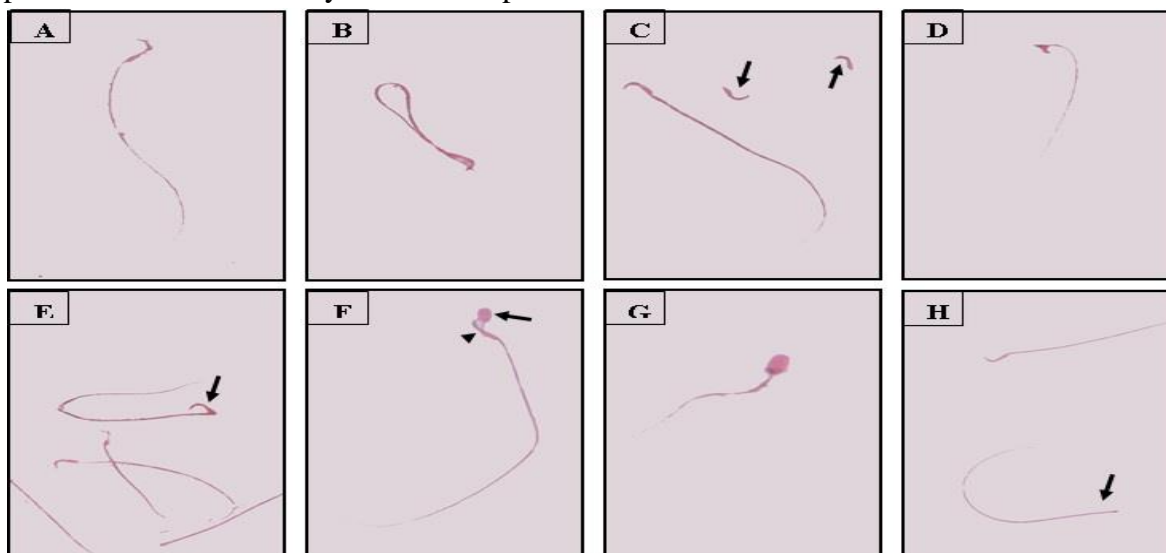


Figure 6: Photomicrography of sperm morphology after the oral administration of CuO NPs in control and treated groups. (A) Normal sperm is composed of a hock-shaped head and tail. (B) Coiled tail sperm (C) Detached sperm head (arrow) (D) Compact sperm head (E) Broken sperm head (arrow) (F) Immature sperm (arrow) overlapping normal sperm (arrowhead) (G) Immature sperm with oval head and short tail (H) Sperm tail without head (arrow). Eosin stain. (Magnification: 40X).

The tendency of the gonadosomatic index to decline after CuO NPs acute oral administration

The gonadosomatic index is the ratio between the testes weight and the total body weight subsequently, it is used as an indicator for reproductive maturity and

performance. Here, all treated groups showed a non-significant decline in GSI compared with the corresponding control in all time points, it is markedly observed with the higher doses. Consequently, almost there is no effect of CuO NPs on GSI and testicular maturity as shown in figure 7.

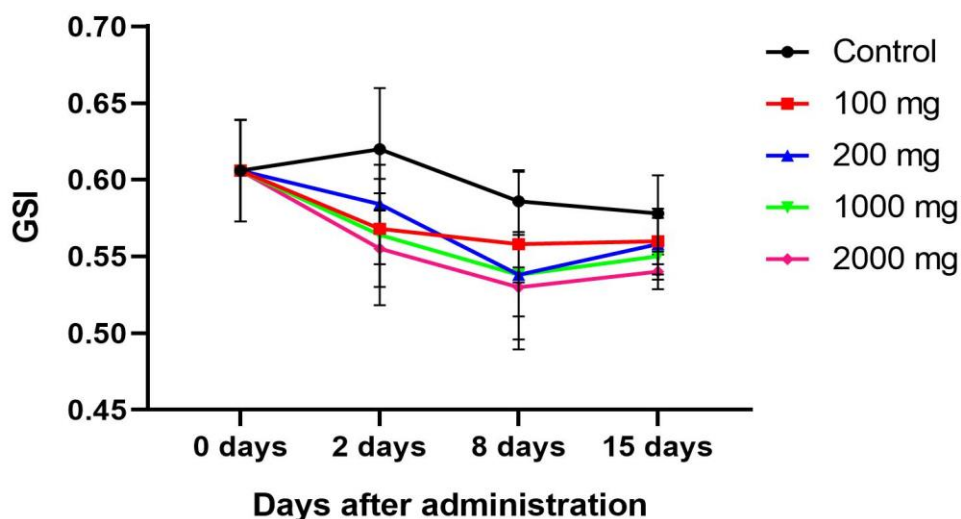


FIGURE 7: GONADOSOMATIC INDEX (GSI) AT DIFFERENT TIME POINTS (2, 8 AND 15 DAYS) AFTER THE ADMINISTRATION OF CuO NPs IN CONTROL AND TREATED GROUPS. DATA ARE EXPRESSED AS THE MEAN \pm SEM ($N = 5$, TWO-WAY ANOVA).

The testicular histological structure is adversely affected by CuO NPs

The testicular tissue specimens were collected from the control and treated groups after 2, 8, and 15 days and processed for histopathological examination. **Figure 8A-C** show normal testicular histological structure with the seminiferous tubules with normal spermatozoa lined with Sertoli cells and normal germ cells with normally arranged Leydig cells. However, **figure 8D-F** illustrate the testes of rats which received 100 mg of CuO NPs with degenerative changes of the germ and Sertoli cells with vacuolation 2 and 8 days after administration. In addition to the aforementioned changes, the same group exhibited thickening of the interstitium with clusters of Leydig cells, besides severe congestion and thickening of the blood

vessel wall after 15 days of administration. Furthermore, the 200 mg-treated groups revealed testicular tissue with degeneration of germ cells, vacuolation, and inflammatory cells infiltration after 2 days. Moreover, the same group after 8 days showed thickening of the interstitium with clusters of Leydig cells beside remarkable congestion and dilatation of the blood vessels and severe edema. Whilst after 15 days, the testicular tissue exhibited atrophied spermatocytes as well edema and thickening of the interstitium with aggregation of Leydig cells (**Figure 8G-I**). The marked histological changes were observed with groups that received high doses of CuO NPs, for instance, **figure 8J-L** revealed testes of rats treated with 1000 mg with atrophied seminiferous tubules with loss of spermatocytes, congestion, and

inflammatory cells infiltration after 2 and 8 days. Besides, the spermatocytes were replaced by vacuoles that are associated with the degeneration of Leydig cells after 15 days. Further, all the previous changes in histological architecture were observed after administration of 2000 mg (**figure 8M-O**) and testicular tissue revealed

degeneration of Sertoli cells and spermatozoa, vacuolation, and severe congestion and dilatation of the blood vessels after 2 and 8 days. In addition, after 15 days, testicular tissue showed atrophied spermatocytes and congestion of the blood vessels with infiltration of round cells.

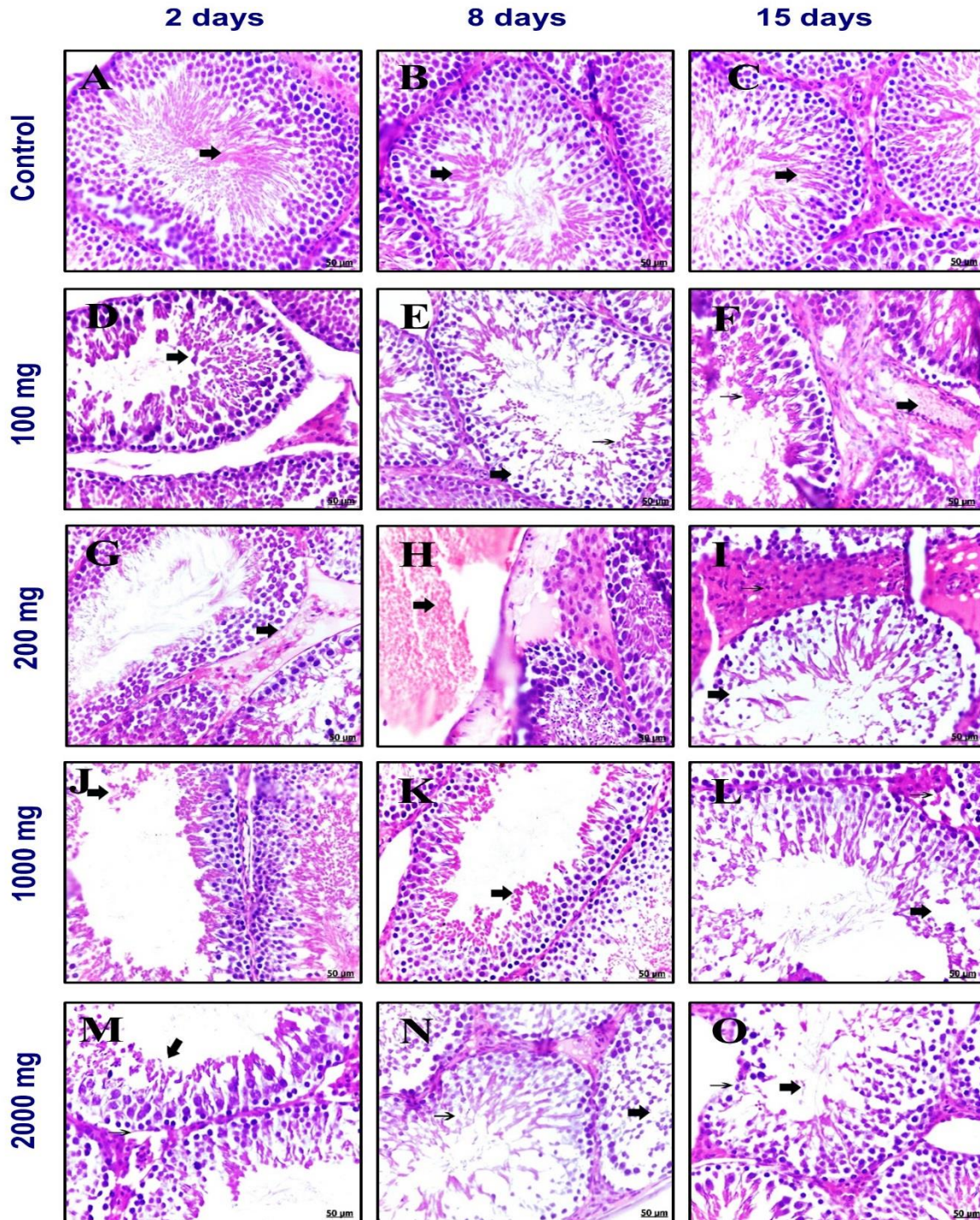


Figure 8: Photomicrograph of the testes in control and treated groups after 2, 8 and 15 days after administration of 100, 200, 1000 and 2000 mg of CuO NPs. (A-C) Teste of control group showing normal histological architecture of the seminiferous tubules with normal spermatozoa lined with Sertoli cells and

normal Leydig cells. (D) Testes of 100 mg-treated group after 2 days show degenerative changes of the Sertoli cells (thick arrow) and spermatozoa as well round cells infiltration. (E) Testes of 100 mg-treated group after 8 days show degenerative changes of the spermatogonia with vacuolation (thick arrow), besides deposition of cell debris and round cells (thin arrow). (F) Testes of 100 mg-treated group after 15 days show degenerative changes of the spermatocytes and Sertoli cells (thin arrow), also thickening of the interstitium with clusters of Leydig cells, besides severe congestion and thickening of the blood vessels wall (thick arrow). (G) Testes of 200 mg-treated group after 2 days show severe edema with expansion of the interstitium (thick arrow) with abundant of Leydig cells. (H) Testes of 200 mg-treated group after 8 days show remarkable congestion and dilatation of the blood vessels (thick arrow) besides severe edema with expansion of the interstitium. (I) Testes of 200 mg-treated group after 15 days show atrophied spermatocytes (thick arrow), as well edema and thickening of the interstitium with aggregation of Leydig cells (thin arrow). (J) Testes of 1000 mg-treated group after 2 days show atrophied seminiferous tubules (thick arrow) with loss of characteristic cells of spermatogenesis. (K) Testes of 1000 mg-treated group after 8 days show atrophied spermatozoa (thick arrow) with round cells infiltration. (L) Testes of 1000 mg-treated group after 15 days show degeneration of the seminiferous tubules with detection of vacuoles replaced spermatocytes (thick arrow), also degeneration of Leydig cells (thin arrow). (M) Testes of 2000 mg-treated group after 2 days degeneration of Sertoli cells (thick arrow) and spermatozoa (thin arrow). (N) Testes of 2000 mg-treated group after 8 days show degeneration of spermatogenic cells with loss of characteristics features (thick arrow), as well vacuolation of the seminiferous tubules (thin arrow). (O) Testes of 2000 mg-treated group after 15 days show degenerative changes of the Sertoli cells (Thick arrow) with atrophied spermatocytes (Thin arrow). (H&E x 400, Scale bar = 50 μ m).

Discussion

The goal of the current study is to clarify the impact of acute oral administration of copper oxide nanoparticles (CuO NPs) on male reproductive performance. Acute CuO NPs harm serum testosterone and sperm characteristics, which is supported by a harmful histological alteration in testicular tissue.

Copper oxide nanoparticles have unique properties that make them useful in various industrial and biomedical applications. For example, they are used as catalysts in various chemical reactions (Gawande *et al.*, 2016), semiconductors (Devi *et al.*, 2014), energy storage devices, such as batteries and supercapacitors (Sahoo *et al.*, 2023), Paints and coatings (Verma and Kumar, 2019) and Sensors (Amini *et al.*, 2021). In addition to industrial applications, CuO NPs are considered one of the most important agents with biomedical uses. They have antimicrobial properties against various bacteria and fungi, making them useful in wound dressings, and disinfectants besides anticancer as they selectively induce

apoptosis of tumor cells and inhibit the growth of cancer cells. Furthermore, copper oxide nanoparticles have been shown to have antioxidant properties depending on the dose and time of exposure and drug delivery due to their ability to penetrate cell membranes and target specific cells (Naz *et al.*, 2023). However, copper oxide nanoparticles have many potential applications, their cellular and biological toxicity, and potential environmental impact are still being studied (Wu *et al.*, 2020; (Naz *et al.*, 2023).

Studies have shown that exposure to copper oxide nanoparticles can have adverse effects on male reproductive health. According to a study carried out by Zheng *et al.* (2023) on male C57BL/6 mice, the current findings are matching with their results that confirm prepubertal exposure to copper oxide nanoparticles is the main cause of decreased testosterone levels. Perturbation of testosterone level is attributed to Leydig cell damage and alteration of steroidogenesis in mouse testes. Furthermore, another investigation discovered that blood testosterone level in men both male and female humans

(Remove it means the effect through adrenal cortex) was inhibited by CuO NPs (Jassim and Salman, 2022). In addition, CuO NPs can pass across the blood-testis barrier (Kim *et al.*, 2005) therefore, they can bioaccumulate in target organs including testicles once they have entered the circulation (Das *et al.*, 2016). It has been demonstrated that CuO NPs are a sensitive target of mammalian testes, and an aggregation of CuO NPs in the male reproductive system can result in serious reproductive damage. In adult mice, CuO NPs can eventually result in aberrant amounts of androgen, decreased sperm counts, and lower semen quality (Souza *et al.*, 2021). For the promotion of spermatogenesis and sperm maturation, normal levels of specific hormones, particularly testosterone, LH, and FSH levels, are crucial. While LH directly drives testosterone production in Leydig cells and the testosterone, FSH indirectly influences the function and activity of Leydig cells by stimulating the Sertoli cells to secrete numerous substances that might impact Leydig cells (Heinrich and DeFalco, 2020). Thus, the most significant endogenous testosterone-producing cells are known as Leydig cells, and the severe decline in testosterone levels in the CuO NPs-treated group suggests that CuO NPs is the main contributor that may cause damage to testicular Leydig cells.

The potential mechanisms by which copper oxide nanoparticles reduce serum testosterone levels are still elusive and not fully understood. However, recent research has indicated that exposure to copper oxide nanoparticles might cause Leydig cell damage with steroidogenesis problems in mice testes, which can lower testosterone levels (Zheng *et al.*, 2023). Another study discovered that varying copper oxide

nanoparticle concentrations change the hormone testosterone's ability to bind to receptors and, therefore, its level in the blood, which has an impact on biological processes that depend on hormone concentration (Jassim and Salman, 2022). It is currently being researched and debated how testosterone levels could be decreased by CuO NPs.

Recent studies have demonstrated that testes are susceptible to oxidative stress because of exposure to copper oxide nanoparticles. Reactive oxygen species (ROS) generation and the body's capacity to detoxify them are out of balance, which causes oxidative stress and cellular damage (Moschini *et al.*, 2023). Even though metal ion dissolution may ultimately contribute to the cytotoxicity caused by CuO NPs, most research tends to blame the harmful impact on the particle's reactivity. Numerous articles have noted that less than half of the overall impact of CuO NPs cytotoxicity is attributable to the extracellularly dispersed copper ions confirming that oxidative stress is a significant factor in cell death (Hanagata *et al.*, 2011; (Wang *et al.*, 2012). Consequently, intracellular copper stimulates the oxidative cascade, which eventually results in DNA damage and cell death by increasing the creation of ROS and depleting glutathione (GSH).

There is evidence to suggest that copper oxide nanoparticles can alter sperm properties. Several studies have investigated the effects of nanoparticles on sperm quality and have found that exposure to certain nanoparticles, including copper oxide nanoparticles, can have negative impacts on sperm parameters. It is important to note that the specific effects of copper oxide nanoparticles on sperm properties may vary depending on factors such as dosage, duration of exposure, and

individual susceptibility. Specifically, they have been shown to induce sperm toxicity and alter sperm characteristics (Vassal *et al.*, 2021). Exposure to copper oxide nanoparticles can lead to a decrease in sperm motility and velocity, as well as a reduction in sperm viability (Garncarek *et al.*, 2022). Furthermore, when exposed to CuO NPs, sperm viability was reduced, mitochondrial activity was hindered, and more reactive oxygen species (ROS) and lipid peroxidation were produced. Additionally, exposure to CuO NPs resulted in morphological changes and DNA damage. These findings, together with the antioxidant rescue studies, point to oxidative stress as the primary cause of the sperm toxicity effects of CuO NPs (Garncarek *et al.*, 2022).

The proposed mechanism of toxicity states that CuO NPs spontaneous induction of ROS and the disruption of the mitochondrial respiratory chain result in the production of ROS, which in turn causes lipid peroxidation and DNA damage, resulting in defective spermatozoa and ultimately causing sperm cytotoxicity. This study, which looked at how CuO NPs affected sea urchin spermatozoa, sheds important light on the mechanism behind the reproductive toxicity caused by CuO NPs (Gallo *et al.*, 2018).

According to Shaoyong *et al.* (2022), exposure to CuO NPs significantly decreased the parameters measuring sperm quality, motility, and movement, as well as the activities of the enzyme antioxidants glutathione peroxidase (GPX), superoxide dismutase (SOD), and catalase (CAT), as well as the parameters measuring energy metabolism and capacitation. Malondialdehyde (MDA) and reactive oxygen species (ROS) levels in human sperm were both noticeably elevated after

exposure to CuO NPs. N-Acetyl-L-Cysteine (NAC) and the Adenosine 5'-monophosphate-activated protein kinase (AMPK) activator both entirely restored the negative effects of CuO NPs on sperm, respectively. By decreasing the AMPK phosphorylation pathway, which is important in activating enzymatic antioxidants, and by raising the levels of ROS and MDA, CuO NPs exposure produced oxidative stress (OS) and harmed sperm function-related metrics. Additionally, CuO NPs exposure lowered sperm capacitation through the OS-mediated cAMP/PKA signaling pathway, which changed from oxidative phosphorylation to glycolysis and decreased ATP levels by inhibiting messenger cAMP production. Protein kinase A (PKA) and tyrosine phosphorylation linked to capacitation were eventually downregulated. Together, our findings point to the possibility that CuO NPs harm sperm through the OS-mediated p-AMPK signaling pathway.

According to the current findings, serum testosterone level decline concomitant with CuO NPs administration by Leydig cells injury and oxidative stress generation subsequently, CuO NPs indirectly impede spermatogenesis and sperm characteristics. Additionally, CuO NPs have been shown to induce oxidative stress and inflammation, which can potentially disrupt hormonal regulation (Jassim and Salman, 2022). A recent study has shown that copper oxide nanoparticles can accumulate in the brain and hamper LH and FSH secretion (Naz *et al.*, 2020). Moreover, exposure to CuO NPs has been shown to clarify a decrease in LH and FSH levels (Sajjad *et al.*, 2023).

The effect of CuO NPson the gonadosomatic index (GSI) has been

studied in a few research articles. GSI is a measure of the reproductive investment of an organism and is calculated as the ratio of gonad weight to body weight. The present results disagree with Farrag *et al.* (2022) who found that exposure to copper nanoparticle fungicides led to an increase in GSI in male redbelly tilapia parallel with testosterone. However, it is important to note that this study did not specifically use CuO NPs, and their study was carried out on fish, not rats. Another study conducted on female rats found that CuO NPs led to reproductive dysfunction by affecting key enzymes of ovarian hormone synthesis and metabolism (Luo *et al.*, 2023). Overall, there is limited information on the specific effects of CuO NPson GSI. Further research is needed to fully understand the extent and mechanisms of these effects.

Exposure to CuO NPs can cause degeneration of seminiferous tubules, spermatocytes, Sertoli cells, and Leydig cells with vacuolation and infiltration of inflammatory cells that are supported the previous studies (Rajabi *et al.*, 2019; (Zheng *et al.*, 2023). Additionally, studies have shown that CuO NPs can disrupt the structure and process of gonadal tissue in male mice, leading to oxidative stress and cellular degradation (Rajabi *et al.*, 2019). Besides, prepubertal exposure to CuO NPs can induce Leydig cell injury with steroidogenesis disorders in mouse testes, leading to decreased testicular weight, disturbed testicular histology, and a reduced number of Leydig cells (Zheng *et al.*, 2023). Histopathological studies have been conducted on testicular tissue samples from male mice exposed to CuO NPs, revealing that CuO NPs can cause significant reductions in testes, epididymal, seminal vesicle, and prostate weights (Al-Musawi *et al.*, 2022).

Conclusion

This study is a trial to bridge the gap between acute single CuO NPs administration and the adverse impact on male reproduction depending on the dose and time elapsed after administration. All doses of CuO NPs used in the current study declined serum testosterone levels, reduced sperm concentration, and elevated abnormal and dead sperm percent. The undesirable effect of CuO NPs extended to involve testicular tissue which depicted marked change in histological architecture such as degeneration of seminiferous tubules, spermatocytes, Sertoli cells, and Leydig cells with vacuolation and infiltration of inflammatory cells.

Reference

- Al-Musawi, M. M. S., Al-Shmgani, H., and Al-Bairuty, G. A. (2022). Histopathological and Biochemical Comparative Study of Copper Oxide Nanoparticles and Copper Sulphate Toxicity in Male Albino Mice Reproductive System. *Int J Biomater*, 2022, 4877637. doi:10.1155/2022/4877637
- Amini, N., Rashidzadeh, B., Amanollahi, N., Maleki, A., Yang, J.-K., and Lee, S.-M. (2021). Application of an electrochemical sensor using copper oxide nanoparticles/polyalizarin yellow R nanocomposite for hydrogen peroxide. *Environmental Science and Pollution Research*, 28(29), 38809-38816. doi:10.1007/s11356-021-13299-6
- Asbrink, S., and Waskowska, A. (1991). CuO: X-ray single-crystal structure determination at 196 K and room temperature. *Journal of Physics Condensed Matter*, 3, 8173-8180. doi:10.1088/0953-8984/3/42/012

- Assy, W., Wasef, M., Abass, M., and Elnegriss, H. (2019). A Study of Short Term Chronic Pulmonary Toxicity, Neurotoxicity and Genotoxicity of Copper Oxide Nanoparticles and The Potential Protective Role of Vitamin E on Adult Male Albino Rats. *Zagazig Journal of Forensic Medicine*, 17(2), 1-18. doi:10.21608/zjfm.2019.10740.1025
- Chen, L., Min, J., and Wang, F. (2022). Copper homeostasis and cuproptosis in health and disease. *Signal Transduct Target Ther*, 7(1), 378. doi:10.1038/s41392-022-01229-y
- D'Souza, U. J. A. (2003). Toxic effects of 5-Fluorouracil on sperm count in wistar rats. *The Malaysian journal of medical sciences : MJMS*, 10(1), 43-45.
- Das, J., Choi, Y.-J., Song, H., and Kim, J.-H. (2016). Potential toxicity of engineered nanoparticles in mammalian germ cells and developing embryos: treatment strategies and anticipated applications of nanoparticles in gene delivery. *Human Reproduction Update*, 22(5), 588-619. doi:10.1093/humupd/dmw020
- Devi, A. B., Moirangthem, D. S., Talukdar, N. C., Devi, M. D., Singh, N. R., and Luwang, M. N. (2014). Novel synthesis and characterization of CuO nanomaterials: Biological applications. *Chinese Chemical Letters*, 25(12), 1615-1619. doi:https://doi.org/10.1016/j.ccllet.2014.07.014
- Esteso, M. C., Soler, A. J., Fernández-Santos, M. R., Quintero-Moreno, A. A., and Garde, J. J. (2006). Functional significance of the sperm head morphometric size and shape for determining freezability in iberian red deer (*Cervus elaphus hispanicus*) epididymal sperm samples. *J Androl*, 27(5), 662-670. doi:10.2164/jandrol.106.000489
- Farrag, M. M. S., Said, R. E., Elmileegy, I. M. H., Abou Khalil, N. S., Abdelallah, E. S. A., El-Sawy, M. F., and Osman, A. G. M. (2022). Effects of penconazole and copper nanoparticle fungicides on redbelly tilapia, *Coptodon zillii* (Gervais, 1848): Reproductive outcomes. *International Journal of Aquatic Biology*, 9(6), 370-382. doi:10.22034/ijab.v9i6.1196
- Gallo, A., Manfra, L., Boni, R., Rotini, A., Migliore, L., and Tosti, E. (2018). Cytotoxicity and genotoxicity of CuO nanoparticles in sea urchin spermatozoa through oxidative stress. *Environ Int*, 118, 325-333. doi:10.1016/j.envint.2018.05.034
- Gamble, M. (2008). 9 - The Hematoxylin and Eosin. In J. D. Bancroft & M. Gamble (Eds.), *Theory and Practice of Histological Techniques (Sixth Edition)* (pp. 121-134). Edinburgh: Churchill Livingstone.
- Garncarek, M., Dziewulska, K., and Kowalska-Górska, M. (2022). The Effect of Copper and Copper Oxide Nanoparticles on Rainbow Trout (*Oncorhynchus mykiss* W.) Spermatozoa Motility after Incubation with Contaminants. *Int J Environ Res Public Health*, 19(14). doi:10.3390/ijerph19148486
- Gawande, M. B., Goswami, A., Felpin, F.-X., Asefa, T., Huang, X., Silva, R., Zou, X., Zboril, R., and Varma, R.

- S. (2016). Cu and Cu-Based Nanoparticles: Synthesis and Applications in Catalysis. *Chemical Reviews*, 116(6), 3722-3811. doi:10.1021/acs.chemrev.5b00482
- Hanagata, N., Zhuang, F., Connolly, S., Li, J., Ogawa, N., and Xu, M. (2011). Molecular responses of human lung epithelial cells to the toxicity of copper oxide nanoparticles inferred from whole genome expression analysis. *ACS Nano*, 5(12), 9326-9338. doi:10.1021/nn202966t
- Hasan, I. M. A., Tawfik, A. R., and Assaf, F. H. (2021). Biosynthesis of α -MoO₃ nanoparticles and its adsorption performance of cadmium from aqueous solutions. *Advances in Natural Sciences: Nanoscience and Nanotechnology*, 12(3), 035007. doi:10.1088/2043-6262/ac2050
- Hasan, I. M. A., Tawfik, A. R., and Assaf, F. H. (2022). GC/MS screening of buckthorn phytochemicals and their use to synthesize ZnO nanoparticles for photocatalytic degradation of malachite green dye in water. *Water Sci Technol*, 85(2), 664-684. doi:10.2166/wst.2021.638
- Heinrich, A., and DeFalco, T. (2020). Essential roles of interstitial cells in testicular development and function. *Andrology*, 8(4), 903-914. doi:https://doi.org/10.1111/andr.12703
- Jassim, S. H., and Salman, T. A. (2022). The Potential of Green-Synthesized Copper Oxide Nanoparticles from Coffee Aqueous Extract to Inhibit Testosterone Hormones. *Egyptian Journal of Chemistry*, 65(4), 395-402. doi:10.21608/ejchem.2021.99308.4620
- Jomova, K., Makova, M., Alomar, S. Y., Alwasel, S. H., Nepovimova, E., Kuca, K., Rhodes, C. J., and Valko, M. (2022). Essential metals in health and disease. *Chemico-Biological Interactions*, 367, 110173. doi:https://doi.org/10.1016/j.cbi.2022.110173
- Kim, J. S., Yoon, T.-J., Yu, K. N., Kim, B. G., Park, S. J., Kim, H. W., Lee, K. H., Park, S. B., Lee, J.-K., and Cho, M. H. (2005). Toxicity and Tissue Distribution of Magnetic Nanoparticles in Mice. *Toxicological Sciences*, 89(1), 338-347. doi:10.1093/toxsci/kfj027
- Kittel, B., Ruehl-Fehlert, C., Morawietz, G., Klapwijk, J., Elwell, M. R., Lenz, B., O'Sullivan, M. G., Roth, D. R., and Wadsworth, P. F. (2004). Revised guides for organ sampling and trimming in rats and mice – Part 2: A joint publication of the RITA1)and NACAD2)groups. *Experimental and Toxicologic Pathology*, 55(6), 413-431. doi:https://doi.org/10.1078/0940-2993-00349
- Kumari, M., and Singh, P. (2013). Study on The Reproductive Organs and Fertility of The Male Mice following Administration of Metronidazole. *International journal of fertility & sterility*, 7(3), 225-238.
- Laurent, S., Forge, D., Port, M., Roch, A., Robic, C., Vander Elst, L., and Muller, R. N. (2008). Magnetic iron oxide nanoparticles: synthesis, stabilization, vectorization, physicochemical characterizations,

- and biological applications. *Chem Rev*, 108(6), 2064-2110. doi:10.1021/cr068445e
- Luo, J., Zhang, M., Deng, Y., Li, H., Bu, Q., Liu, R., Yu, J., Liu, S., Zeng, Z., Sun, W., Gui, G., Qian, X., and Li, Y. (2023). Copper nanoparticles lead to reproductive dysfunction by affecting key enzymes of ovarian hormone synthesis and metabolism in female rats. *Ecotoxicology and Environmental Safety*, 254, 114704. doi:https://doi.org/10.1016/j.ecoenv.2023.114704
- Maulana, I., Fasya, D., and Ginting, B. (2022). Biosynthesis of Cu nanoparticles using *Polyalthia longifolia* roots extracts for antibacterial, antioxidant and cytotoxicity applications. *Materials Technology*, 37(13), 2517-2521. doi:10.1080/10667857.2022.2044217
- Mohamed, R., Hasan, I. M. A., Maher, Z. M., and Ahmed, H. (2023). Copper Oxide Nanoparticles suppress the liver and kidney function and decrease antioxidant defense in adult male rats after acute oral administration. *SVU-International Journal of Veterinary Sciences*, 6(3), 93-113. doi:10.21608/svu.2023.218969.1279
- Moschini, E., Colombo, G., Chirico, G., Capitani, G., Dalle-Donne, I., and Mantecca, P. (2023). Biological mechanism of cell oxidative stress and death during short-term exposure to nano CuO. *Scientific Reports*, 13(1), 2326. doi:10.1038/s41598-023-28958-6
- Naz, S., Gul, A., and Zia, M. (2020). Toxicity of copper oxide nanoparticles: a review study. *IET Nanobiotechnol*, 14(1), 1-13. doi:10.1049/iet-nbt.2019.0176
- Naz, S., Gul, A., Zia, M., and Javed, R. (2023). Synthesis, biomedical applications, and toxicity of CuO nanoparticles. *Appl Microbiol Biotechnol*, 107(4), 1039-1061. doi:10.1007/s00253-023-12364-z
- OECD. (2001). *OECD GUIDELINE FOR TESTING OF CHEMICALS. OECD/OCDE, Adopted 17th December; 1-14.*
- Rajabi, S., Shahbazi, Fatemeh, Noori, A., and Karshenas, R. (2019). Investigation of the Toxic Effects of Copper Oxide Nanoparticles on the Structure of Gonadal Tissue in Male. *Experimental animal Biology*, 7(4), 117-124. doi:10.30473/eab.2019.6399
- Sahoo, K., Varshney, N., Das, T., Mahto, S. K., and Kumar, M. (2023). Copper oxide nanoparticle: multiple functionalities in photothermal therapy and electrochemical energy storage. *Applied Nanoscience*, 13(8), 5537-5558. doi:10.1007/s13204-023-02768-8
- Sajjad, H., Sajjad, A., Haya, R. T., Khan, M. M., and Zia, M. (2023). Copper oxide nanoparticles: In vitro and in vivo toxicity, mechanisms of action and factors influencing their toxicology. *Comparative Biochemistry and Physiology Part C: Toxicology & Pharmacology*, 271, 109682. doi:https://doi.org/10.1016/j.cbpc.2023.109682
- Samrot, A. V., and Noel Richard Prakash, L. X. (2023). Nanoparticles Induced Oxidative Damage in Reproductive System and Role of Antioxidants on

- the Induced Toxicity. *Life*, 13(3), 767. Retrieved from <https://www.mdpi.com/2075-1729/13/3/767>
- Seed, J., Chapin, R. E., Clegg, E. D., Dostal, L. A., Foote, R. H., Hurtt, M. E., Klinefelter, G. R., Makris, S. L., Perreault, S. D., Schrader, S., Seyler, D., Sprando, R., Treinen, K. A., Veeramachaneni, D. N., and Wise, L. D. (1996). Methods for assessing sperm motility, morphology, and counts in the rat, rabbit, and dog: a consensus report. ILSI Risk Science Institute Expert Working Group on Sperm Evaluation. *Reprod Toxicol*, 10(3), 237-244. doi:10.1016/0890-6238(96)00028-7
- Shaoyong, W., Xu, B., Liu, Y., Pan, B., Wang, Y., and Jin, M. (2022). Exposure to Copper Oxide Nanoparticles Causes Human Infertility Risk and Damages the Quality of the Human Sperm Via the 5'Amp-Activated Protein Kinase-Mediated Signaling Pathway in Vitro. *SSRN Electronic Journal*. doi:10.2139/ssrn.4052477
- Souza, M. R., Mazaro-Costa, R., and Rocha, T. L. (2021). Can nanomaterials induce reproductive toxicity in male mammals? A historical and critical review. *Science of The Total Environment*, 769, 144354. doi:<https://doi.org/10.1016/j.scitotenv.2020.144354>
- Srinivasulu, K., and Changamma, C. J. I. J. o. P. S. (2017). A Study on the Effect of Ocimum sanctum (Linn.) Leaf Extract and Ursolic Acid on Spermatogenesis in Male Rats. *Indian Journal of Pharmaceutical Sciences* 79(1), 158-163.
- Thommes, M., Kaneko, K., Neimark, A. V., Olivier, J. P., Rodriguez-Reinoso, F., Rouquerol, J., and Sing, K. S. W. (2015). Physisorption of gases, with special reference to the evaluation of surface area and pore size distribution (IUPAC Technical Report). *Pure and Applied Chemistry*, 87(9-10), 1051-1069. doi:doi:10.1515/pac-2014-1117
- Tietz, N. W. (1995). *Clinical Guide to Laboratory Tests*. 3rd ed. W.B. Saunders, Co., Philadelphia, 578-580.
- Vassal, M., Rebelo, S., and Pereira, M. L. (2021). Metal Oxide Nanoparticles: Evidence of Adverse Effects on the Male Reproductive System. *International journal of molecular sciences*, 22(15). doi:10.3390/ijms22158061
- Verma, N., and Kumar, N. (2019). Synthesis and Biomedical Applications of Copper Oxide Nanoparticles: An Expanding Horizon. *ACS Biomaterials Science & Engineering*, 5(3), 1170-1188. doi:10.1021/acsbiomaterials.8b01092
- Vinothkanna, A., Mathivanan, K., Ananth, S., Ma, Y., and Sekar, S. (2022). Biosynthesis of copper oxide nanoparticles using Rubia cordifolia bark extract: characterization, antibacterial, antioxidant, larvicidal and photocatalytic activities. *Environ Sci Pollut Res Int*. doi:10.1007/s11356-022-18996-4
- Wang, Z., Li, N., Zhao, J., White, J. C., Qu, P., and Xing, B. (2012). CuO nanoparticle interaction with human epithelial cells: cellular uptake,

- location, export, and genotoxicity. *Chem Res Toxicol*, 25(7), 1512-1521. doi:10.1021/tx3002093
- Wu, F., Harper, B. J., Crandon, L. E., and Harper, S. L. (2020). Assessment of Cu and CuO nanoparticle ecological responses using laboratory small-scale microcosms. *Environmental Science: Nano*, 7(1), 105-115. doi:10.1039/c9en01026b
- Wyrobek, A. J., and Bruce, W. R. (1975). Chemical induction of sperm abnormalities in mice. *Proceedings of the National Academy of Sciences of the United States of America*, 72(11), 4425-4429. doi:10.1073/pnas.72.11.4425
- Zheng, X., Chen, J., Kang, L., Wei, Y., Wu, Y., Hong, Y., Wang, X., Li, D., Shen, L., Long, C., Wei, G., and Wu, S. (2023). Prepubertal exposure to copper oxide nanoparticles induces Leydig cell injury with steroidogenesis disorders in mouse testes. *Biochemical and Biophysical Research Communications*, 654, 62-72. doi:https://doi.org/10.1016/j.bbrc.2023.02.067